united nations
educational, scientific
and cultural
organization

international atomic
energy agency

the
abdus salam
international centre for theoretical physics

SMR 1521/4

AUTUMN COLLEGE ON PLASMA PHYSICS

13 October - 7 November 2003

Selective Decays: Coherent Structures on the Cheap

D. C. Montgomery

Dartmouth College,
Dept. of Physics and Astronomy
Hanover, USA

SELECTIVE DECAYS: COHERENT STRUCTURES ON THE CHEAP

They result from the rapid turbulent decay of one ideal invariant relative to another. But why should this happen?

An answer is to be found in the direction of spectral transfer (in wave number) in "cascade" processes: direct or inverse cascades.

To appreciate how, in detail, this may be so, it is necessary to review notions of cascades and inverse cascades.

NAVIER-STOKES AND MHD EQS.

(Dimensionless "Alfvénic" Units)

$$\frac{\partial \underset{\sim}{v}}{\partial t} + \underset{\sim}{v} \cdot \nabla \underset{\sim}{v} = -\nabla p + \nu \nabla^2 \underset{\sim}{v} + \underset{\sim}{j} \times \underset{\sim}{B}$$

$$\nabla \cdot \underset{\sim}{v} = 0$$

$$\nabla \cdot \underset{\sim}{B} = 0$$

$$\frac{\partial \underset{\sim}{B}}{\partial t} + \underset{\sim}{v} \cdot \nabla \underset{\sim}{B} = \underset{\sim}{B} \cdot \nabla \underset{\sim}{v} + \eta \nabla^2 \underset{\sim}{B}$$

$$\nabla \times \underset{\sim}{B} = \underset{\sim}{j}$$

Periodic boundary conditions:

$$\underset{\sim}{v} = \sum_{\underset{\sim}{k}} \underset{\sim}{v}(\underset{\sim}{k}, t) \exp(i \underset{\sim}{k} \cdot \underset{\sim}{x})$$

$$\underset{\sim}{k} = \frac{2\pi}{L} \underset{\sim}{n} = \frac{2\pi}{L} (n_x, n_y, n_z)$$

$$L \longrightarrow \infty$$

$$\underset{\sim}{v} \xrightarrow[L\to\infty]{} \int d^3k \; \underset{\sim}{v}(\underset{\sim}{k},t)\exp(i\underset{\sim}{k}\cdot\underset{\sim}{x})$$

$$\underset{\sim}{k}\cdot\underset{\sim}{v}(\underset{\sim}{k},t) = 0$$

$$\left(\frac{\partial}{\partial t} + \nu k^2\right) v_i(\underset{\sim}{k},t)$$

$$= M_{ijk}(\underset{\sim}{k}) \sum_{\underset{\sim}{l}+\underset{\sim}{q}=\underset{\sim}{k}} v_j(\underset{\sim}{l})\, v_k(\underset{\sim}{q})$$

↑ (integral, if $L\to\infty$)

GENERIC FORM:

$$\frac{dX_i}{dt} + \nu_i X_i = \sum_{jk} C_{ijk} X_j X_k$$

NONLINEAR TERMS ARE >> LINEAR ONES, BY FACTORS OF THE REYNOLDS NUMBER.

IDEAL INVARIANTS ($\nu = 0$):

3D:
$$\begin{cases} E = \frac{1}{2}\int \underset{\sim}{v}^2 d^3x \longrightarrow \frac{1}{2}\sum_{\underset{\sim}{k}} |\underset{\sim}{v}(\underset{\sim}{k},t)|^2 \\ H = \frac{1}{2}\int \underset{\sim}{v}\cdot\underset{\sim}{\omega}\, d^3x \longrightarrow \frac{1}{2}\sum_{\underset{\sim}{k}} \underset{\sim}{v}^*(\underset{\sim}{k},t)\cdot(i\underset{\sim}{k}\times\underset{\sim}{v}(\underset{\sim}{k},t)) \end{cases}$$

2D:
$$\begin{cases} E = \frac{1}{2}\int \underset{\sim}{v}^2 d^2x \\ \Omega = \frac{1}{2}\int \omega^2 d^2x \end{cases}$$

GENERIC FORM (IN FOURIER SPACE):

$$E = \frac{1}{2}\sum_i X_i^2$$

$$\frac{dE}{dt} = \sum_{ijk} C_{ijk} X_i X_j X_k = 0 \quad , \quad \text{all } X_i$$

$$\Rightarrow C_{ijk} + C_{jki} + C_{kij} = 0, \text{ and}$$

QUADRATIC INVARIANTS SURVIVE TRUNCATION IN FOURIER SPACE.

TRUNCATED FOURIER EXPANSION OF EULER DYNAMICS CAN BE APPROACHED AS A PROBLEM IN EQUILIBRIUM STATISTICAL MECHANICS, BECAUSE A LIOUVILLE THEOREM IS OBEYED (KRAICHNAN, 1950s).

e.g., 3D NAVIER STOKES

$$D_{eq.}(X_1 X_2 \cdots X_N) = C^{-\beta E - \alpha H} \times \text{const.}$$

Lagrange Multipliers $\left\{ \begin{array}{l} \alpha = \alpha(\langle E \rangle, \langle H \rangle, N) \\ \beta = \beta(\langle E \rangle, \langle H \rangle, N) \end{array} \right.$

$$\langle H \rangle = 0 \Rightarrow \alpha = 0$$

$$D_{eq.} = \text{const.}\, e^{-\beta E}$$

$$\langle |\underset{\sim}{u}(\underset{\sim}{k})|^2 \rangle \propto \frac{1}{\beta}, \text{ all } \underset{\sim}{k},$$

AN EQUIPARTION SPECTRUM

(NOTHING LIKE REALLIFE, WITH $\nu \neq 0$)

3D NS (Continued): Kolmogorov 1941

$$\mathcal{E}(k) \propto 4\pi k^2 \langle |\underset{\sim}{v}(\underset{\sim}{k})|^2 \rangle \quad \text{(ISOTROPIC)}$$

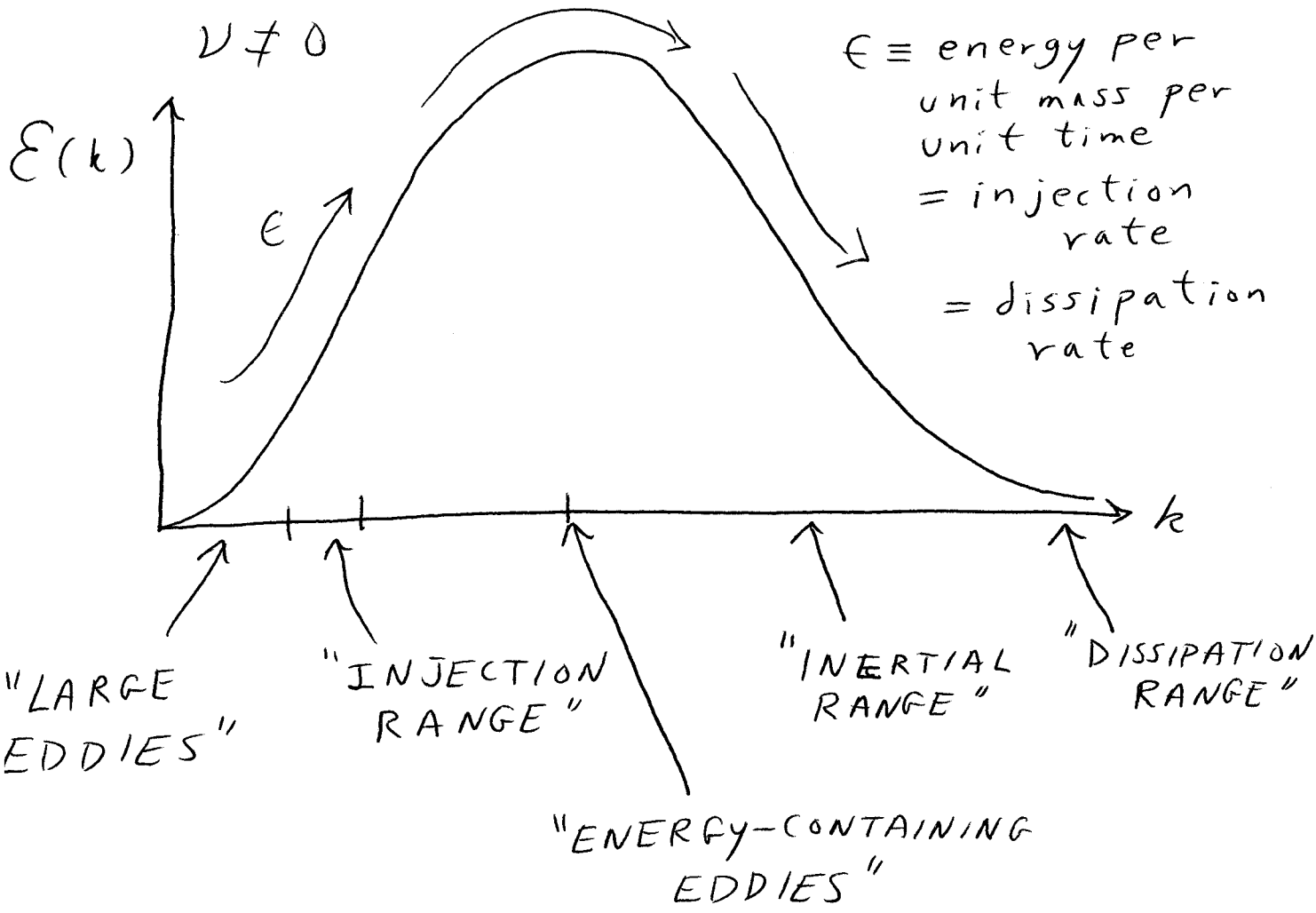

$$\mathcal{E}(k) = \text{const.}\ \epsilon^r k^s \quad \text{(IN INERTIAL RANGE)}$$

DIMENSIONAL ANALYSIS: $r = 2/3$, $s = -5/3$

$$\boxed{\mathcal{E}(k) = C_{Ko}\, \epsilon^{2/3} k^{-5/3}}$$

3D NS (Continued)

Dimensional analysis also gives

$$k_D = \text{"dissipation wave number"}$$
$$\cong (\epsilon/\nu^3)^{1/4}$$

The absolute equilibrium Gibbs ensemble would have given

$$\mathcal{E}(k) \propto k^2,$$

totally at variance with reality.

2D NS:

$$D_{eq.} = \text{const.}\ e^{-\beta E - \alpha \Omega}$$

$$\langle |\underset{\sim}{U}(\underset{\sim}{k})|^2 \rangle \propto \frac{1}{\beta + \alpha k^2}$$

(this is positive, but either α or β may be negative)

Interesting behavior as $k_{max} \to \infty$ (Kraichnan 1967):

HOLD $\langle E \rangle$, $\langle \Omega \rangle$ FIXED, Let N and $k_{max} \longrightarrow \infty$:

$$\beta \to -\infty$$
$$\alpha \to +\infty$$

ALL THE ENERGY CONDENSES IN k_{min}.

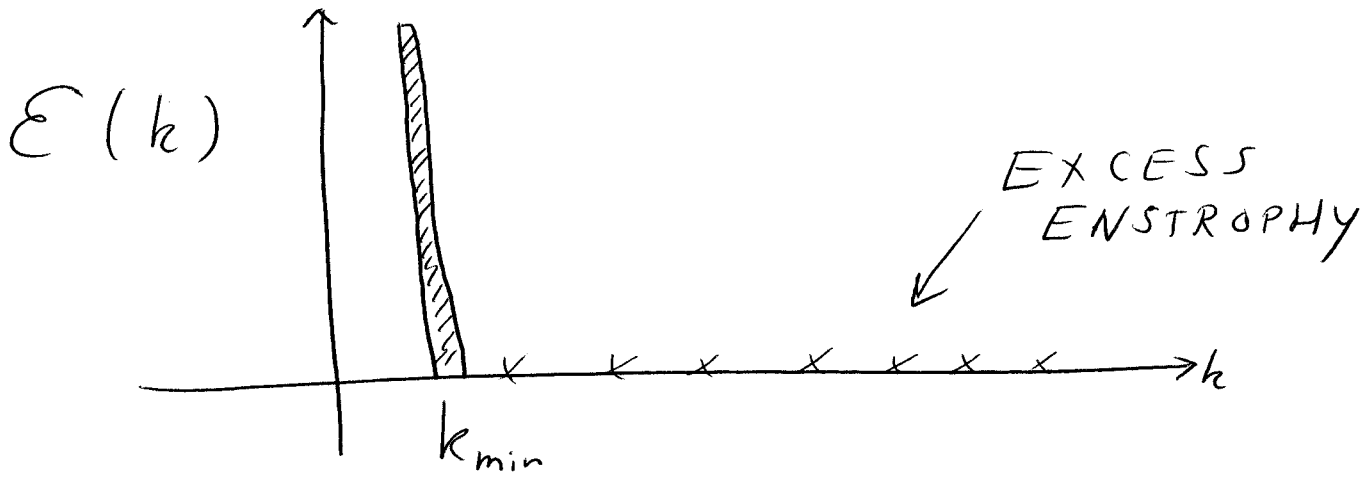

KRAICHNAN CONJECTURED A DUAL CASCADE, IF INJECTION WAVENUMBERS ARE $\gg k_{min}$ AND $\ll k_D$.

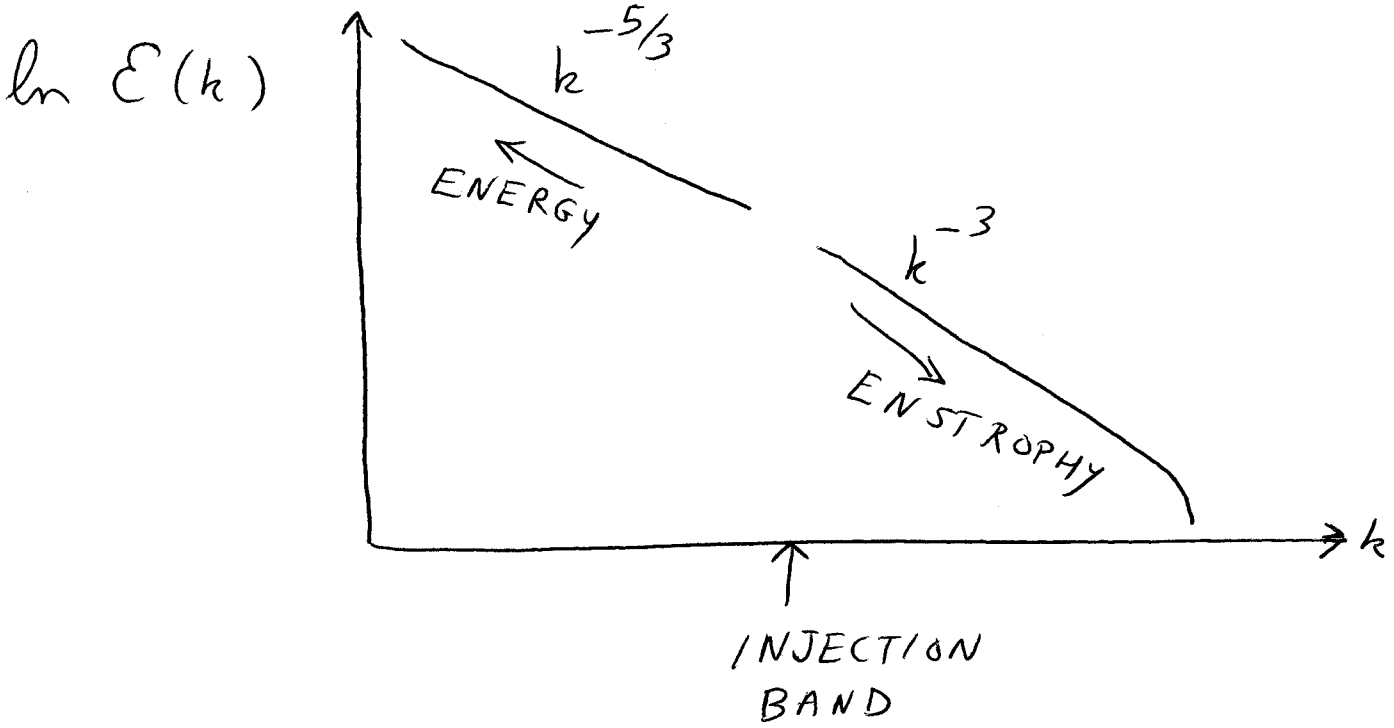

ENERGY IN FACT PILES UP IN LONGEST WAVELENGTHS ALLOWED BY BOUNDARY CONDITIONS, LIMITED BY ITS OWN DISSIPATION RATE (HOSSAIN et al, 1983).

$$k_D \text{ (for enstrophy)} \propto \frac{|d\Omega/dt|^{1/6}}{\nu^{1/2}}$$

POWER LAWS ARE COMPUTABLE ONLY BY ARTIFICIAL MEANS — SINKS AT BOTH HIGH AND LOW k. BUT QUALITATIVE BEHAVIOR IS BEYOND DISPUTE.

THERE ARE IMPLICATIONS FOR DECAYING 2D NS TURBULENCE (NO FORCING OR INJECTION)

THEOREM:

$$\frac{d}{dt}\frac{\Omega}{E} \leq 0,$$

$= 0$ ONLY IF SPECTRUM IS MONOCHROMATIC IN $|\underset{\sim}{k}|$.

ALL $k > k_{min}$ MONOCHROMATIC SPECTRA ARE UNSTABLE

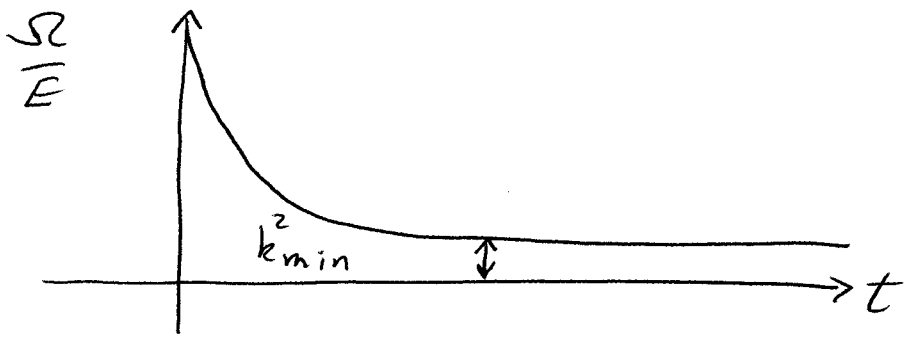

"FINAL" STATE INVOLVES ONLY $k = k_{min}$ COMPONENTS ("SELECTIVE DECAY")

IN A PERIODIC BOX OF EDGE 2π,

THE FINAL DECAYED STATE IS A

MIXTURE OF $\underset{\sim}{k} = (1,0), (0,1), (-1,0), (0,-1)$,

TYPICALLY A DIPOLE:

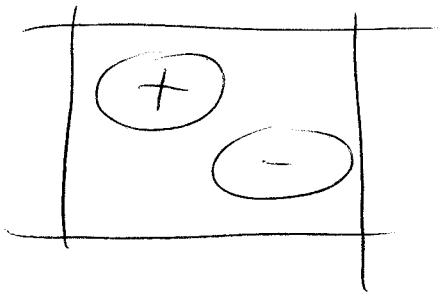

MATTHAEUS + MONTGOMERY, ANN. NY. ACAD. SCI. 357, 203 (1980).

ONLY AT HIGHER REYNOLDS NUMBER (LOWER ν) DID IT BECOME APPARENT THAT MAXIMUM ENTROPY STATE (SINH-POISSON) BECAME RELEVANT LONG BEFORE Ω/E REACHED k^2_{min}.

MHD ANALOGUES ARE TO BE EXPECTED IN ANY SITUATION WHERE INVERSE CASCADES MAY BE POSSIBLE IN THE PRESENCE OF DRIVING.

	2D MHD	3D MHD
Inversely-Cascadable Ideal Invariant	Mean-square vector potential	Magnetic Helicity
Directly-Cascadable Ideal Invariant*	Energy, Cross-Helicity	Energy, Cross-Helicity

* An exceptional case occurs when the initial cross-helicity,

$$\int \underset{\sim}{v} \cdot \underset{\sim}{B}\, d^2x \quad \text{or} \quad \int \underset{\sim}{v} \cdot \underset{\sim}{B}\, d^3x$$

IS LARGE.

2D MHD:

Minimize $E \equiv \frac{1}{2} \int (\underset{\sim}{v}^2 + \underset{\sim}{B}^2) d^2x$

subject to $A \equiv \frac{1}{2} \int A_z^2 \, d^2x$

approximately constant,

$$\underset{\sim}{B} = \nabla \times (\hat{e}_z A_z(x, y, t)).$$

3D MHD:

Minimize $E \equiv \frac{1}{2} \int (\underset{\sim}{v}^2 + \underset{\sim}{B}^2) d^3x$

subject to $H \equiv \int \underset{\sim}{A} \cdot \underset{\sim}{B} \, d^3x$

approximately constant

$$\underset{\sim}{B} = \nabla \times \underset{\sim}{A}(x, y, z, t)$$

$$\nabla \cdot \underset{\sim}{A} = 0$$

IN BOTH CASES, THE KINETIC ENERGY GOES AWAY, AND THE $\underset{\sim}{B}$-FIELD IS OBTAINED FROM THE EULER-LAGRANGE EQUATIONS

$$\nabla^2 A_z + \lambda^2 A_z = 0 \qquad (2D)$$

$$\nabla \times \underset{\sim}{B} = \lambda \underset{\sim}{B}. \qquad (3D)$$

THESE STATEMENTS APPLY TO PERIODIC BOUNDARY CONDITIONS. MORE REALISTIC BOUNDARY CONDITIONS MAY MANDATE MORE CONSTRAINTS:

e.g., MAGNETIC FLUX DOWN A CYLINDER.

EACH CONSTRAINT WILL ADD A COMPLEXITY TO THE EULER-LAGRANGE EQUATION.

MANY VARIATIONS EXIST, AND MOST OF THEM ARE INTERESTING.

THE QUESTION IS, DOES IT REALLY HAPPEN? THE ANSWER IS YES, TO A FIRST APPROXIMATION:

TING et al, PHYS. FLUIDS 29, 3261 (1986).

RIYOPOULOS et al, PHYS. FLUIDS 25, 107 (1982).

DAHLBURG et al, PHYS. REV. LETT. 57, 428 (1986)
J. PLASMA PHYS. 37, 299 (1987).

HOWEVER, AT HIGH ENOUGH RESOLUTION AND HIGH ENOUGH VALUES OF THE REYNOLDS-LIKE NUMBERS, THE PROCESS STOPS SHORT OF THE FULLY RELAXED STATE. SEE:

KINNEY, McWILLIAMS, and TAJIMA
PHYS. PLASMAS 2, 3623 (1995).

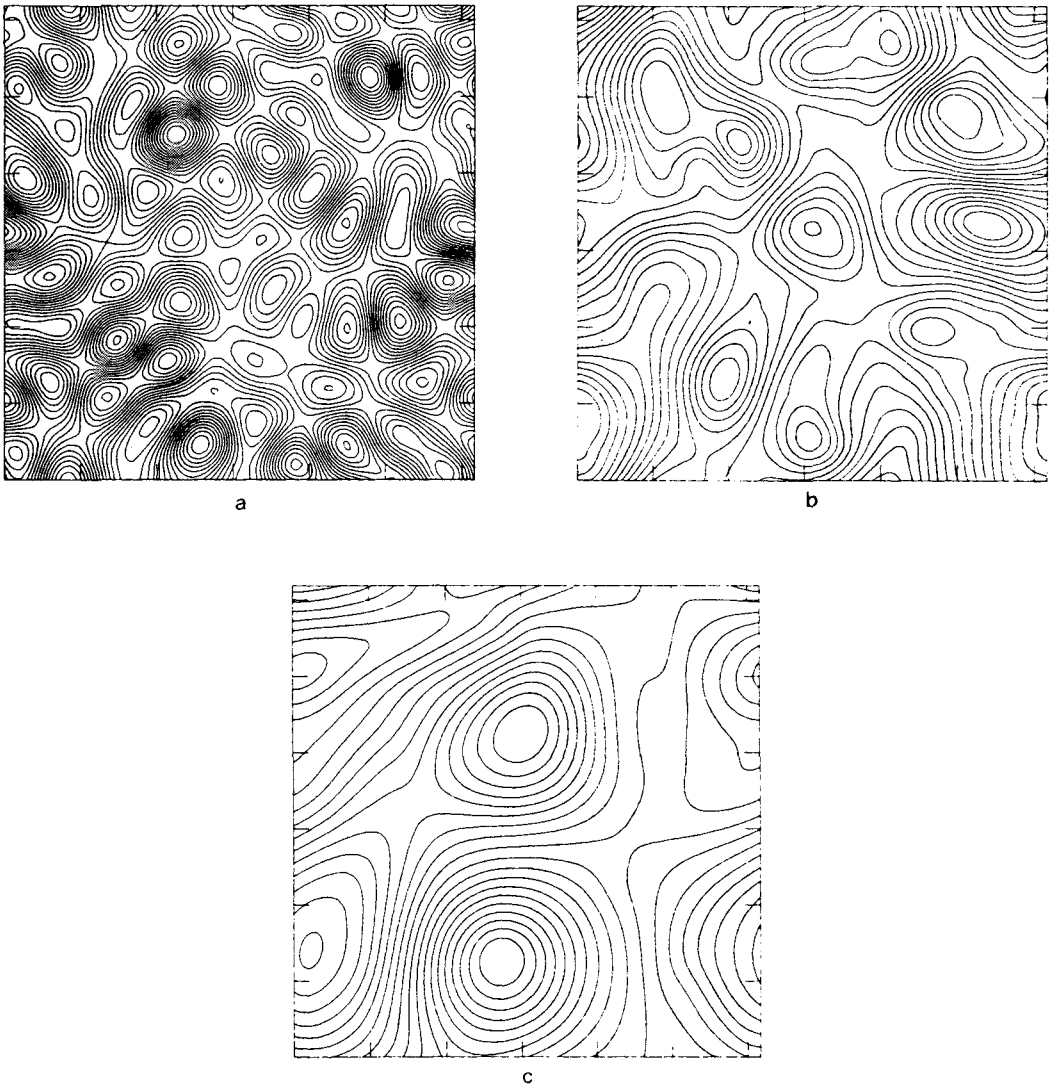

FIGURE 3. Contour plots of the stream function ψ for the two-dimensional Navier-Stokes simulation. Lines of constant ψ are parallel to $\mathbf{v}$, and the magnitude of $\mathbf{v}$ is inversely proportional to the line spacing. Shown are streamlines at $t = 0$ (*a*), $t = 1000$ (*b*), and $t = 3000$ (*c*).

plots of constant stream function ψ (recall that $\nabla^2\psi = -\omega$), showing the progressive disappearance of the high k components and the gradual smoothing of the streamlines.

Other runs have been carried out with $R = 200$ and 1000, with similar results.

TWO-DIMENSIONAL MHD

An incompressible conducting fluid obeys a more complicated but very similar set of equations.[32] First, an electric current force term gets added into (**1**):

$$\frac{\partial \mathbf{v}}{\partial t} + \mathbf{v} \cdot \nabla \mathbf{v} = -\nabla p + \mathbf{j} \times \mathbf{B} + \frac{1}{R}\nabla^2 \mathbf{v}. \qquad (15)$$

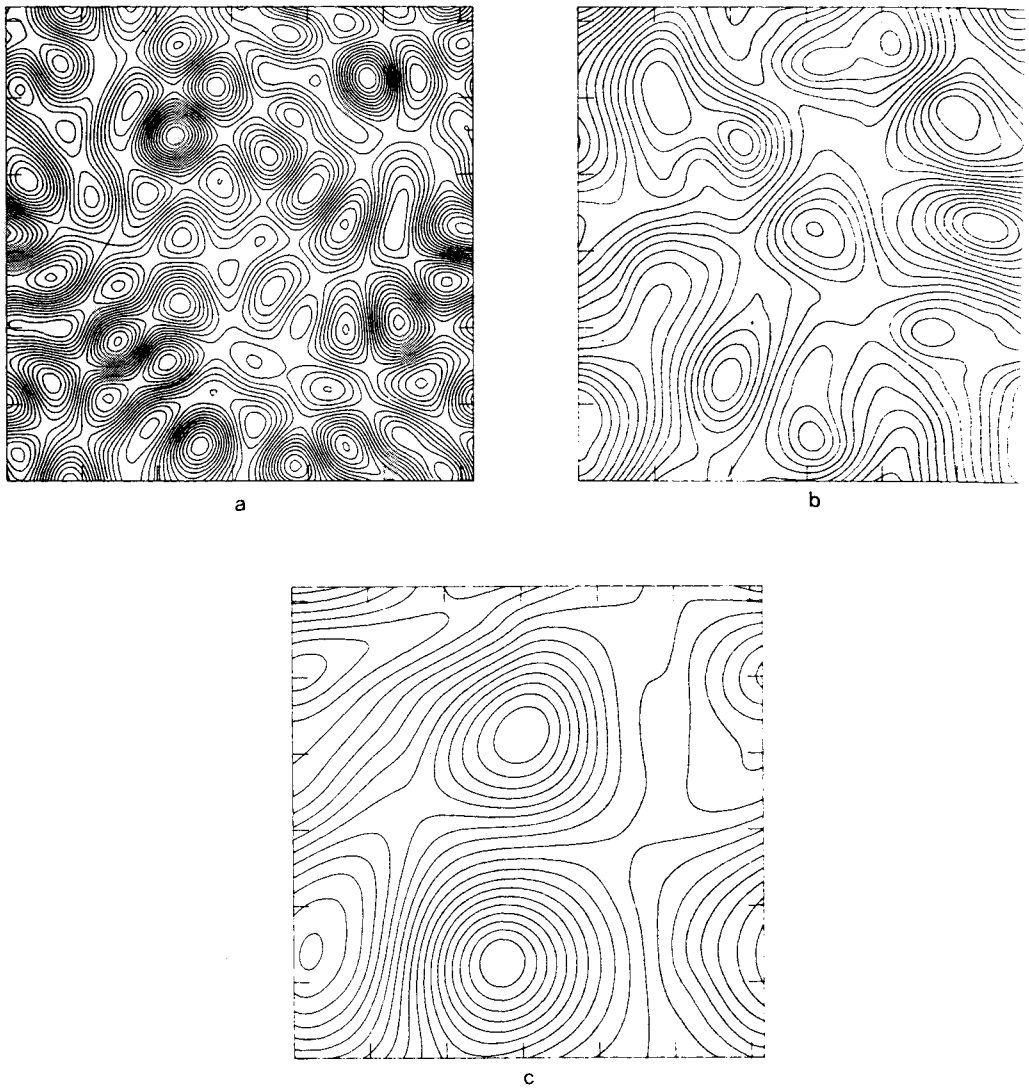

FIGURE 3. Contour plots of the stream function ψ for the two-dimensional Navier-Sto simulation. Lines of constant ψ are parallel to $\mathbf{v}$, and the magnitude of $\mathbf{v}$ is inversely proportio to the line spacing. Shown are streamlines at $t = 0$ (*a*), $t = 1000$ (*b*), and $t = 3000$ (*c*).

plots of constant stream function ψ (recall that $\nabla^2\psi = -\omega$), showing the progress disappearance of the high k components and the gradual smoothing of the strea lines.

Other runs have been carried out with $R = 200$ and 1000, with similar resul

TWO-DIMENSIONAL MHD

An incompressible conducting fluid obeys a more complicated but very similar of equations.[32] First, an electric current force term gets added into (**1**):

$$\frac{\partial \mathbf{v}}{\partial t} + \mathbf{v} \cdot \nabla \mathbf{v} = -\nabla p + \mathbf{j} \times \mathbf{B} + \frac{1}{R}\nabla^2 \mathbf{v}.$$

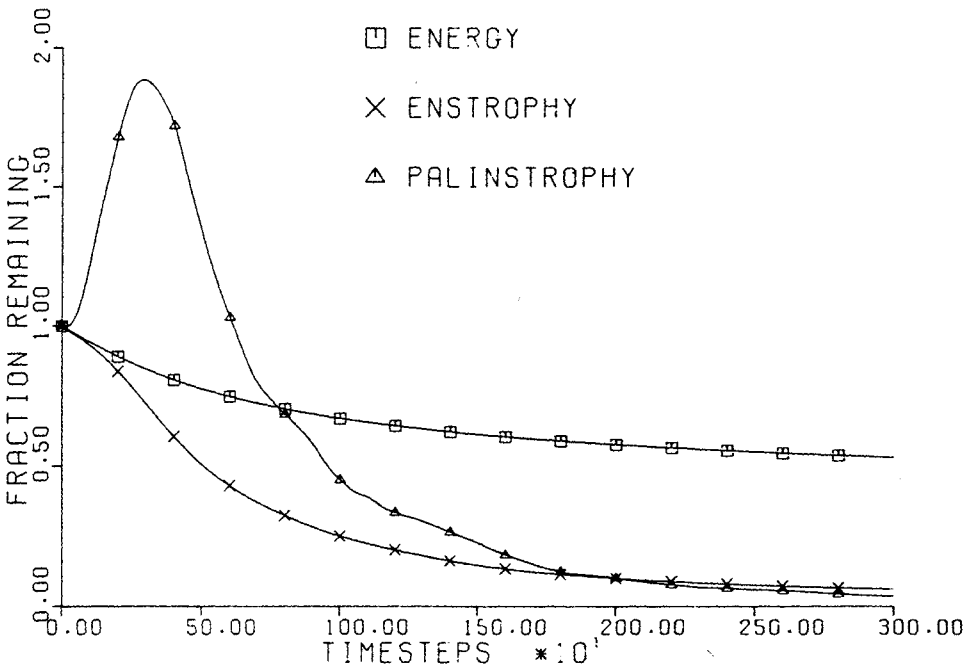

FIGURE 1b. The time history of energy (E), enstrophy (Ω), and palinstrophy (P) are shown, each normalized to its initial value. The dramatic increase in P occurs in one or two turnover times of the large eddies; this is entirely due to the nonlinear interactions. The enhancement of P causes Ω to decay rapidly, which, in turn, lessens the rate of energy decay.

$$\frac{\mathrm{d}}{\mathrm{d}t} H_m \equiv \frac{\mathrm{d}}{\mathrm{d}t} \int \mathbf{A} \cdot \mathbf{B} \mathrm{d}^3x = -\frac{2}{R_m} \int \mathbf{B} \cdot \mathbf{j} \mathrm{d}^3x. \tag{24}$$

The quantity $H_m \equiv \int \mathbf{A} \cdot \mathbf{B} \mathrm{d}^3x$ is called the *magnetic helicity* and is basically a measure of the amount of electric current that flows along the magnetic field.

Once again, we consider what might happen as R, $R_m \rightarrow \infty$. On the basis of the consideration that the dissipation rate might remain finite for those quantities whose decay integrands contain the highest number of spatial derivatives, it is again natural to assume that energy might decay while magnetic helicity is conserved.

In this discussion, as in the section that discusses two-dimensional MHD, the assumption that cross helicity, H_c, decays on the same time scale as the energy E is

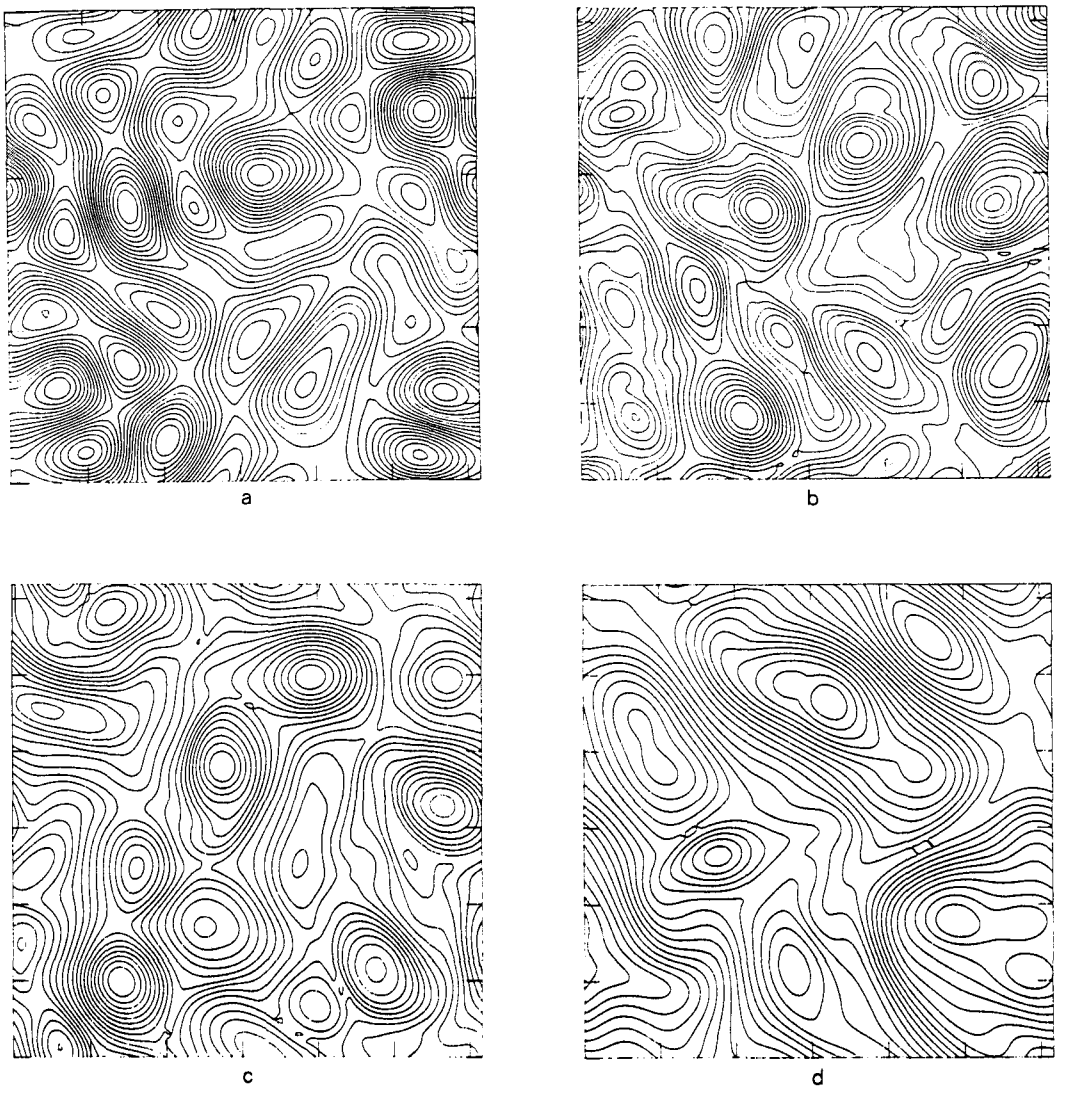

FIGURE 7. Contour plots of the vector potential field, $a(\mathbf{x})$. Shown are lines of $a(\mathbf{x})$ = const. Since $\mathbf{B} \cdot \nabla a = 0$, these are instantaneous magnetic field line plots, with the field line strength inversely proportional to the line spacing. The plots are for times $t = 0$ (a), $t = 500$ (b), $t = 1000$ (c), and $t = 2500$ (d).

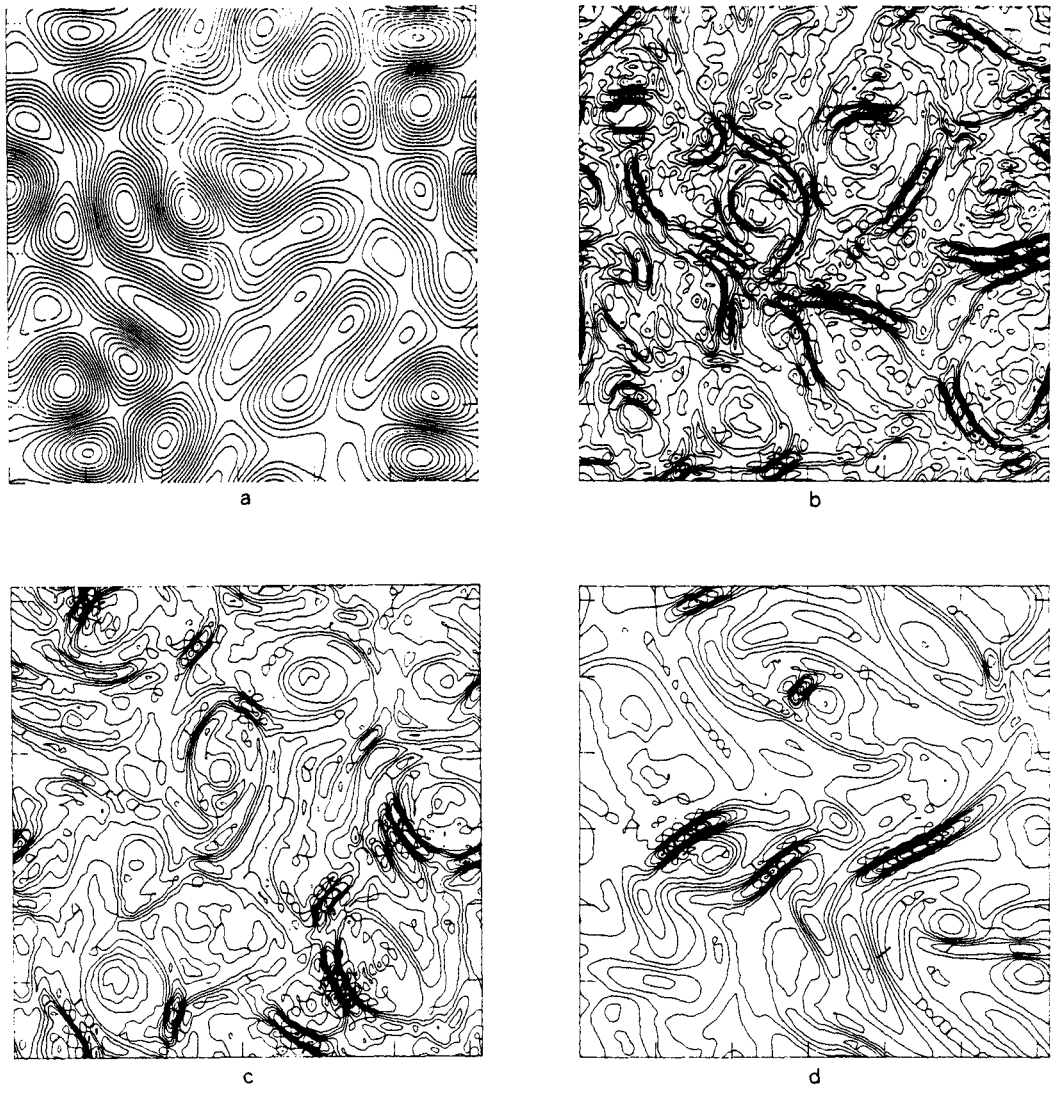

FIGURE 8. Contour plots of the electric current, $j(\mathbf{x})$. The plots are times $t = 0$ (a), $t = 500$ (b), $t = 1000$ (c), and $t = 2500$ (d). Complicated small scale dynamics involving localization of current are apparent.

implicit. There are some subtleties, however, because the decay of H_c and H_m are not necessarily monotonic: the right-hand sides of (**20**) and (**24**) are not negative definite. Recently, there has been a suggestion by Grappin, Frisch, Leorat, and Pouquet that cross helicity may decay *less* rapidly than energy,[34] which, if true, will alter the conclusions presented here. If energy were to decay, but not H_c *or* H_m, then the decay could be to a finite-velocity equilibrium that might support a pressure gradient, as will be seen after the following considerations are made clear.

Suppose first that E were to decay to its minimum value compatible with conservation of H_m, unconstrained by any conservation or partial conservation of H_c. Then the kinetic energy would be zero and the resulting variational problem would involve magnetic quantities alone.

The minimum of E, subject to the constraint $H_m = \text{const.}$, leads to the Euler

$$\frac{dA}{dt} \equiv \frac{d}{dt}\int a^2 d^2x = -\frac{2}{R_m}\int B^2 d^2x, \tag{19}$$

and

$$\frac{dH_c}{dt} \equiv \frac{d}{dt}\int \mathbf{v}\cdot\mathbf{B}d^2x = -\left(\frac{1}{R}+\frac{1}{R_m}\right)\int \boldsymbol{\omega}\cdot\mathbf{j}d^2x, \tag{20}$$

The three nondissipative invariants E, A, and H_c, are the total energy, the mean square vector potential, and the "cross helicity," respectively. The possibilities for selective decays as R, $R_m \to \infty$ are more numerous, but we might explore first the

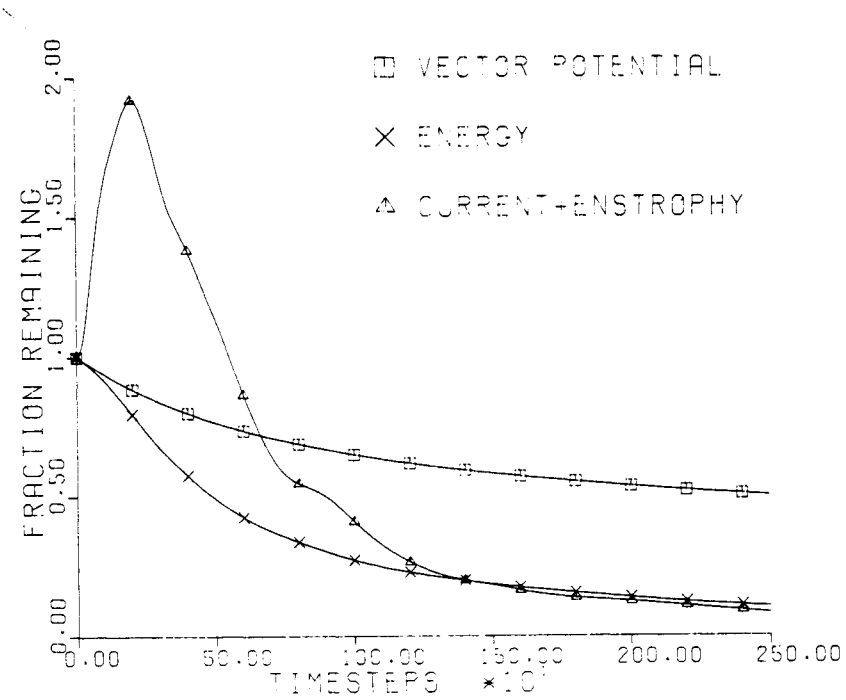

FIGURE 5. The time evolution of mean square vector potential, energy, and the sum of enstrophy and mean square current, each divided by its initial value, for the MHD simulation with $R = R_m = 200$.

consequences of assuming decay of E to its minimum value compatible with conservation of A. The spectral representations of **(18)**, **(19)**, and **(20)**, by analogy with the Navier-Stokes considerations of the previous section, suggest a dissipation range in which the spectra of ω and j peak at higher and higher values in order to keep dE/dt of 0(1).

If E is minimized subject to conservation of A, then the kinetic energy will have all been dissipated and the magnetic energy will have decayed to its minimum value compatible with the initial value of A. The Euler equation for this minimum problem is

$$\nabla^2 a - \lambda a = 0, \tag{21}$$

where λ is a Lagrange multiplier, which, for periodic boundary conditions, must be

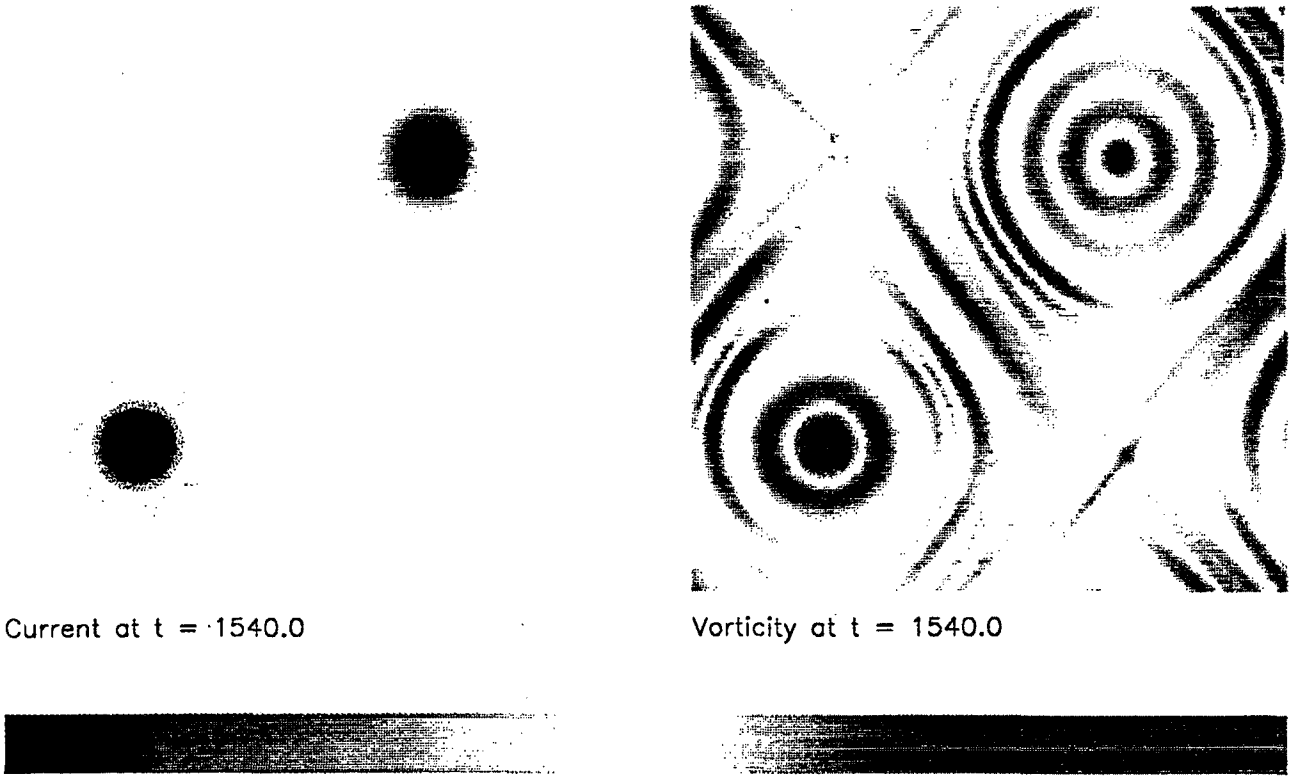

FIG. 21. Current and vorticity fields from an $N=256$ solution at $t=1540$.

By $t\sim 300$ in this solution, the last coalescence between vortices has taken place, and the remaining dynamics are primarily dissipative. Figure 21 shows the current and vorticity at $t=1540$, after most of the nonaxisymmetric transients from the coalescence have been removed. To our knowledge, this is the first report of such an end-state for high Reynolds number MHD turbulence. The current is in a magnetic dipole state, with one vortex of either sign, but there is a noticeable asymmetry. The positive (blue) vortex is larger and stronger and is surrounded by a negative ring, which the negative vortex lacks. The vorticity extrema have the same sign, but also differ in size and strength.

It is possible to express a stationary state of 2D MHD in terms of functions of the vector potential

$$\psi=\Psi(a),$$
$$j=J(a)+\Psi'\zeta. \tag{23}$$

In figure 22(a), we show a scatter plot of ψ vs. a in the final state. There remains an appreciable amount of noise which is dying away very slowly, but ψ does appear to be converging to a single-valued function of a. Notice that the magnitude of ψ is much smaller than a because of the conservation of A. Figure 22(b) shows scatter plots of j and ζ vs. a, in which both fields are nearly single-valued functions of a. The magnitude of ζ relative to j is much greater than that of ψ relative to a. At $t=300$, when the dynamics begin to be dominated by dissipation, the vorticity in the stronger vortex is 16% of the current. The vorticity, however, dissipates more rapidly due to being distributed over smaller scales, and the ratio of extrema in the strong vortex has decreased to 8% by the time of this figure.

In predicting the end-state of turbulent evolution, one constraint on the functions Ψ and J is that the state must be stable. Sufficient conditions for nonlinear stability in 2D MHD have been derived by Lyapunov techniques.[39] For a purely magnetic state, this condition is $J'\leqslant 0$. Our state clearly has regions where $J'>0$, and so does not satisfy these stability conditions, even when finite Ψ and ζ are taken into account. Maximum entropy statistical arguments also give rise to predictions of fluid end-states. In the case of neutral turbulence, one prediction is that $\zeta=-|\gamma_0|\sinh(|\gamma_1|\psi)$,[40] or that ψ satisfies the "sinh-Poisson" equation. Because solutions of neutral 2D turbulence at very long times inevitably evolve towards a final dipole state, with a single vortex of either sign,[41,42] the final state is always qualitatively similar to a sinh-Poisson state. Discrepancies may arise in the relative positioning of the vortices or from differences in size and shapes of the final vortices, though the latter can be accommodated by refinements to the entropy argument at the cost of increasing the number of free parameters.[43]

Because of the formation and interaction of magnetic vortices, MHD should always reach a magnetic dipole in its final state. Furthermore, the relative positions of the vortices is predetermined due to the repulsive force between them. Therefore, statistical predictions of MHD[44] should enjoy the

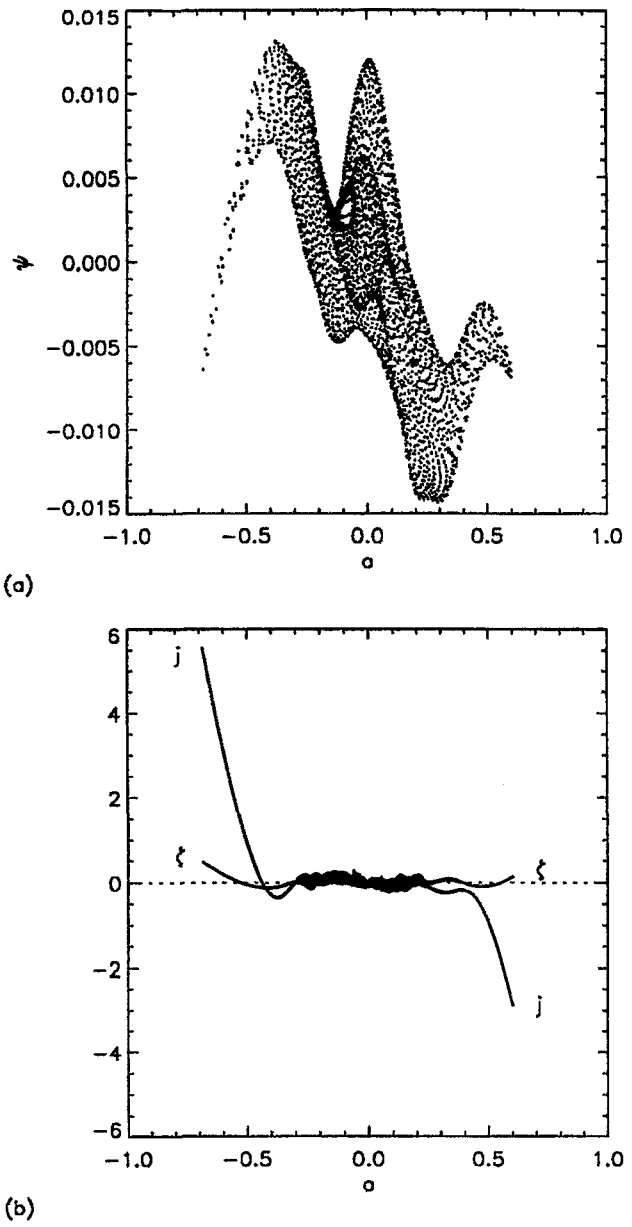

FIG. 22. Scatter plots of ψ vs. a (a) and j and ζ vs. a (b) at $t=1540$. For clarity, a uniform subset of the points are shown in (a).

same qualitative agreement with the final states of particular solutions. However, our state clearly does not resemble the "selective decay" predictions[6] $\psi \propto a$, $j \propto a$, and there remains a significant degree of asymmetry between the final vortices. We believe that the specific shape of the final state of a particular solution is sensitive to its initial conditions, which determine the initial sizes and strengths of the magnetic vortices as well as, ultimately, their subsequent interaction history. During the course of interacting with other vortices, the final survivors may or may not acquire rings and may end up with a range of sizes and strengths. The vorticity profile of a final vortex is particularly sensitive to initial conditions because the vorticity is carried nearly passively by structures whose interaction is primarily magnetic.

V. CONCLUSIONS

We have computed solutions of decaying 2D MHD at high Reynolds number for a variety of initial conditions with initial spectra which are peaked in a narrow band at a wavenumber well separated from the minimum wavenumber. We have observed a long-lived period of self-similar evolution which occurs for all Reynolds numbers considered and all initial configurations with magnetic energy above a certain threshold. The self-similar evolution is characterized by power-law time dependencies of second-order moments, fixed ratios of enstrophy production conversion and dissipation, and an energy partition at intermediate scales in which $E_v(k) \approx 0.4 E_B(k)$. Measures of the intermittency of the current field and local measures of alignment between the magnetic and velocity field at mid-to-small scales grow consistently during the self-similar evolution. The fluid is dominated by coherent magnetic vortices, which control the turbulent cascade indirectly through current sheets generated during close encounters between the vortices.

When the initial ratio of kinetic to magnetic energy is sufficiently large ($\geqslant 1000$), the dynamics are that of a neutral fluid with the magnetic potential, a, a passive scalar. When the initial ratio is 100, the magnetic field is active, but mostly at small scales. Spectrum shapes are close to those in the magnetically passive cases, and the dynamics are predominantly neutral, but the enstrophy production rate continues to be significant, and dissipation is strongly enhanced over the magnetically passive solutions. All other solutions eventually reach magnetic dominance at all scales. Solutions with initial energy ratios $\leqslant 1$ quickly reach such a state while those with ratios >1 and <100 reach it only after undergoing a slower phase of spectrum adjustment.

During the self-similar evolution, the kinetic and magnetic enstrophies decay with the same power-law time dependence. The energies do not decay at the same rate; there is consistent loss of E_v relative to E_B. This is because energies are strongly influenced (in different ways) by the finite size of the system, but the enstrophies are not. The enstrophy budget may be broken down into three simultaneous processes: production of magnetic enstrophy, conversion of magnetic to kinetic enstrophy, and dissipation of magnetic and kinetic enstrophies. The rates of all these processes may be fit to the form $Gt^{-1.9} + G_1 t^{-2.3}$ in which the coefficients G are such that the $t^{-1.9}$ terms give no contribution to $\dot{W}_j$ and $\dot{W}_\zeta$, which consequently evolve as $t^{-2.3}$. This suggests a powerful foreground process in which enstrophy is produced and dissipated with no net contribution to the total enstrophy. Overwhelmed by this is a subtler background process which actually determines the net enstrophy evolution.

The fluid is intermittent; probability distributions of current and vorticity are exponential rather than Gaussian. Furthermore, the intermittency of the current grows during the self-similar evolution. Alignment of the velocity and magnetic fields at large scales is weak, but alignment at smaller scales (i.e., between current and vorticity gradients) grows along with the degree of intermittency. The spectrum shape acquires a $k^{-3/2}$ shape near the time of maximum dissipation but afterwards steepens considerably towards a $k^{-5/2}$ depen-

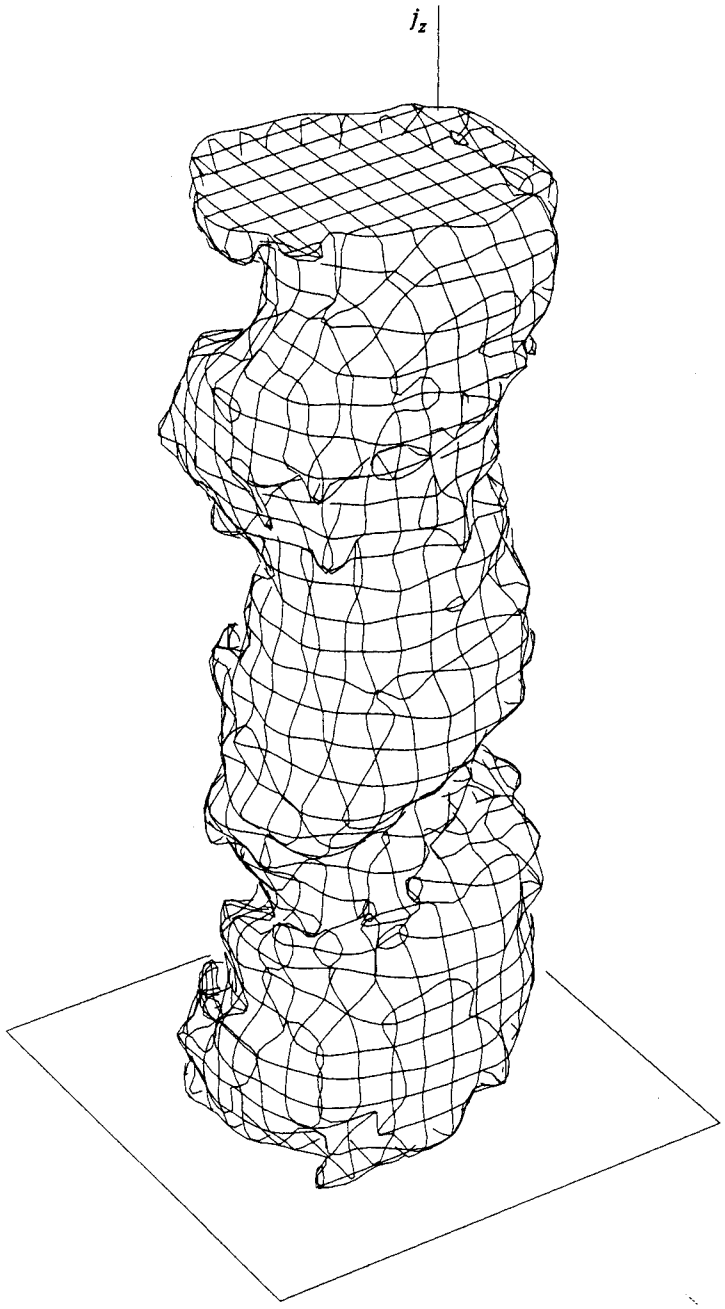

FIGURE 7. Three-dimensional plot of $0{\cdot}45 \times j_{z\max}(x, y, t = 74{\cdot}4)$.

magnetic) spectra are plotted *vs.* wavenumber in a somewhat unconventional way. The energy spectrum $E(k'_x, k'_y, k'_z)$, say, is summed over all mode numbers $k'_x, k'_y \equiv j, k$ in the two poloidal directions and over all values of k'_z up to $k'_z = k_z$. The result has to be a monotonically increasing function of k_z which may be called the 'accumulated spectrum'. A similar accumulated spectrum can be computed for dissipation, upon multiplying the magnetic energy spectral contributions by $2(k'^2_x + k'^2_y + k'^2_z)/S$ and summing again. A computation which had resolved all dynamically-participating wavenumbers would show a perfectly flat accumulated spectrum immediately to the left of the maximum k_z (in this case, 32). Figure 11 shows, at time $t = 19{\cdot}7$, the accumulated energy and dissipation spectra for the $S = 250$ run under discussion (for accumulated

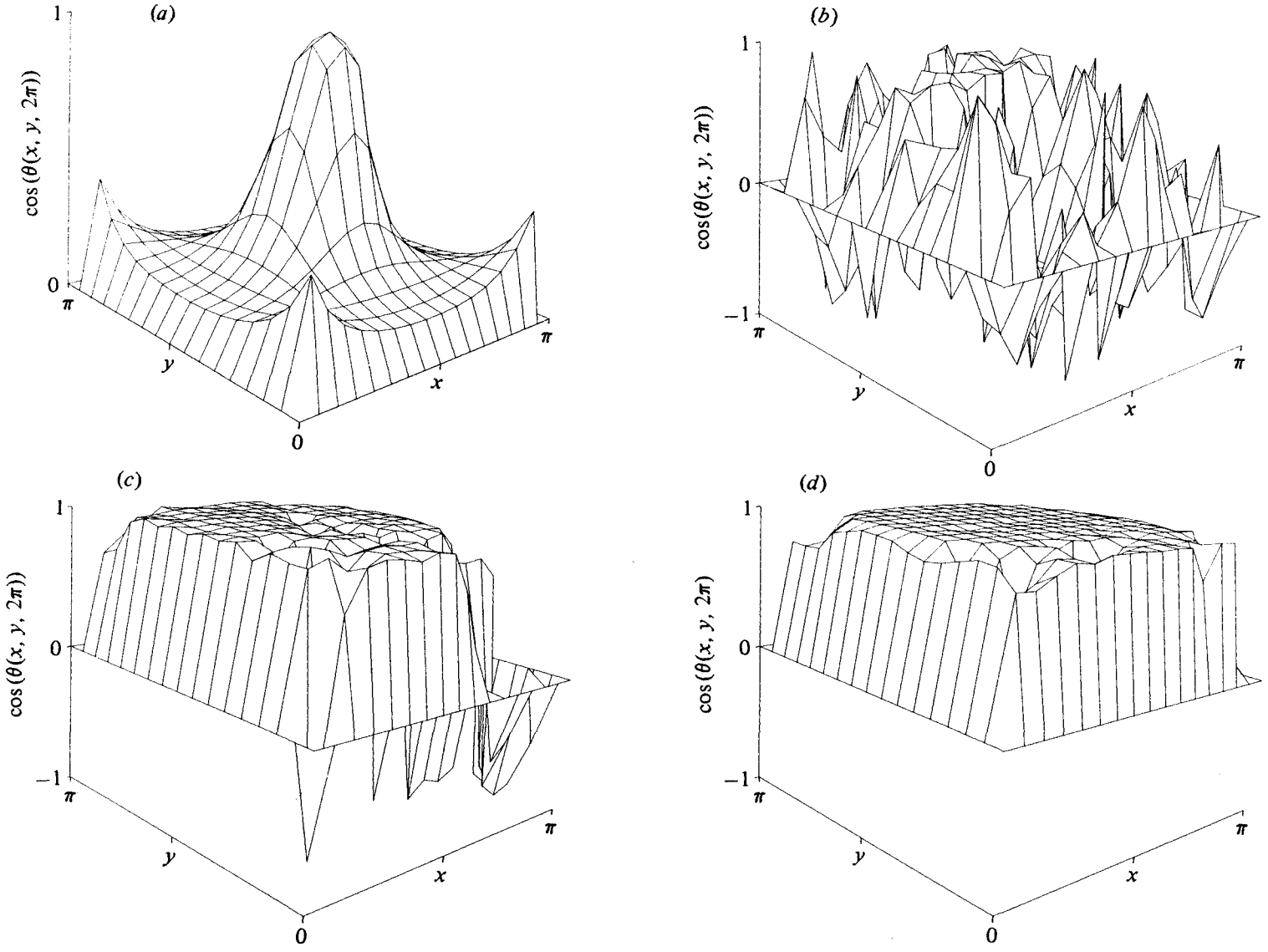

FIGURE 9. (*a*) Three-dimensional perspective plot in the (x, y) plane at $z = 2\pi$ of the alignment cosine, $\mathbf{j} \cdot \mathbf{B}_{\text{tot}}/(jB_{\text{tot}})$. (*a*) $t = 0$, (*b*) 12·0, (*c*) 39·3, (*d*) 74·4; relaxation toward a force-free state is apparent.

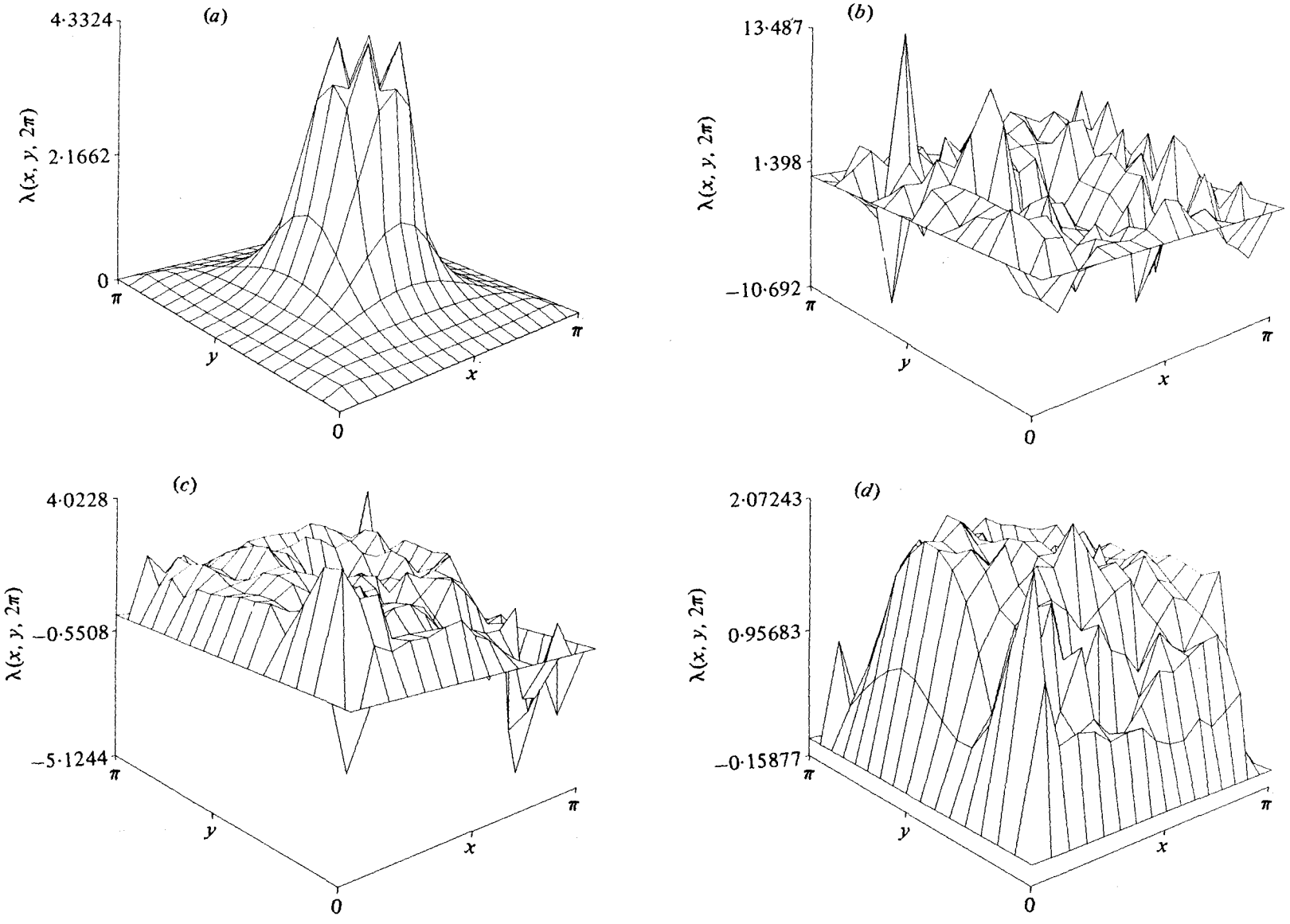

FIGURE 10. Three-dimensional perspective plot in the (x, y) plane at $z = 2\pi$ of $\lambda \equiv \mathbf{j} \cdot \mathbf{B}_{\text{tot}}/(B_{\text{tot}}^2)$.
(*a*) $t = 0$, (*b*) 12·0, (*c*) 39·3, (*d*) 74·4.

SUMMARY:

SELECTIVE DECAYS, THE RAPID DISSIPATION OF A DIRECTLY-CASCADABLE IDEAL INVARIANT AT SHORT WAVELENGTHS SIMULTANEOUSLY WITH THE APPROXIMATE CONSERVATION OF AN INVERSELEY CASCADABLE ONE, WILL LEAD RELIABLY TO QUALITATIVE PREDICTIONS OF COHERENT STRUCTURES WHICH HAVE LONG LIVES IN FLUIDS AND MAGNETO-FLUIDS.

HOWEVER, THEY USUALLY FALL SHORT OF AGREEMENT WITH THE DETAILS OF THE PREDICTIONS. REAL-LIFE BOUNDARY CONDITIONS ARE OFTEN ONE INTRUSION. PROBABILISTIC CONSIDERATIONS (AS IN "MAXIMUM ENTROPY" VS. "SELECTIVE DECAY" DIFFERENCES IN 2D NS) ARE ANOTHER. THE LATTER REQUIRES MORE CAREFUL THINKING IN CONNECTION WITH MHD.